

Effect of annealing on d.c. conductivity of V_2O_5 –SnO–TeO₂ glasses

HIDETSUGU MORI, HIRONOBU SAKATA

Department of Applied Chemistry, Tokai University, 1117, Kitakaname, Hiratsuka, Kanagawa 259-12, Japan

The d.c. conductivity (σ) of V_2O_5 –SnO–TeO₂ glasses prepared by the press–quenching method was studied at temperatures from room temperature (RT) to 473 K, and the effect of annealing on σ was investigated. The conductivity of $50V_2O_5 \cdot 20SnO \cdot 30TeO_2$ glass was determined to be $3.98 \times 10^{-4} \text{ S cm}^{-1}$ at 473 K and was unchanged for annealing (6–48 h) at 493 K, lower than $T_g = 501 \text{ K}$, while its density increased with annealing time. These glasses were found to be n-type semiconductors, and the conduction was confirmed to be due to adiabatic small polaron hopping for $V_2O_5 \geq 50 \text{ mol } \%$, and non-adiabatic for $V_2O_5 < 50 \text{ mol } \%$. The activation energy for conduction, W , decreased with annealing time. Variations in oxygen molar volume of the glasses with annealing time inferred a change in glass structure, from loosely to closely packed, resulting in a decrease in vanadium ion spacing with annealing. This caused an increase in the polaron band width, producing a decrease in polaron hopping energy and W . The effect of annealing time on the density of $50V_2O_5 \cdot 20SnO \cdot 30TeO_2$ glass was explained adequately by Winter's formula.

1. Introduction

Electrical conduction of glasses containing transition metal oxides (TMO) has been understood in terms of the small polaron hopping (SPH) model [1–7]. Recently, tellurite glasses [3–7] with TMO have been extensively studied. We investigated electrical conduction for V_2O_5 –SnO–TeO₂ glasses [6] at temperatures between room temperature (RT) and 473 K, and concluded that the conduction was attributed to be adiabatic SPH for $V_2O_5 \geq 50 \text{ mol } \%$, but non-adiabatic SPH for $V_2O_5 < 50 \text{ mol } \%$. A d.c. conductivity study of V_2O_5 –SnO–TeO₂ annealed glass systems [7] at low temperatures (RT–200 K) was also carried out and variable-range hopping conduction [8] was observed at $T < \text{RT}$. On the other hand, electrical properties of crystallized glasses have been investigated [9–11]. For crystallized glasses in the Nb_2O_5 – V_2O_5 – P_2O_5 system [9], the d.c. conductivity increased remarkably with increasing annealing time (0–48 h) from $\sigma = 10^{-6}$ – $10^{-3} \text{ S cm}^{-1}$ at 503 K; the activation energy for conduction increased from 0.50 to 0.20 eV, higher than that of non-annealed glasses [9]. However, we found no literature on the effect of annealing on electrical conductivity of TMO-containing glasses. In the present work, we annealed press–quenched glasses in the V_2O_5 –SnO–TeO₂ system [6] in air and examined effects of annealing on SPH conduction and glass density.

2. Experimental procedure

The process for the preparation of glass samples is described elsewhere [6, 7]. Regent grade 99.9% V_2O_5 ,

99.9% SnO and 99.99% TeO₂ were mixed for 20 min in prescribed composition and a batch (5 g) was melted in air in a porcelain crucible with in an electric furnace at 750 °C for 1 h. The melt was poured onto a copper plate and rapidly quenched by pressing with another copper plate. The glass samples of 5 g and 1.0 mm thickness and 4 cm² were obtained. The glass transition temperature, T_g , was measured by differential thermal analysis (DTA). Based on T_g data ($T_g = 228 \text{ °C}$ for $50V_2O_5 \cdot 20SnO \cdot 30TeO_2$ glass), the annealing temperature was set to 220 °C. Annealing times were 6, 12, 24 and 48 h. The amorphous nature of the samples was checked by X-ray diffraction. The four-point probe method was employed to determine d.c. electrical resistivity from RT to 473 K, where 1 μA d.c. current was applied during the measurement. D.c. conductivity on the same glass samples in different runs agreed within 0.1%. Samples of the same glass composition from different batches gave agreement within 5% for room temperature conductivity. The density of the glasses was measured at 293 K by Gay–Lussac pycnometry using toluene. The density on the same sample in different runs agreed within 0.01% of error.

3. Results

The X-ray diffractograms of the annealed glasses showed no trace of crystallinity. T_g of the present glasses was 224 °C for $60V_2O_5 \cdot 10SnO \cdot 30TeO_2$ and 228 °C for $50V_2O_5 \cdot 20SnO \cdot 30TeO_2$, respectively [6]. The glasses were found to be n-type semiconductors as a result of thermoelectric power measurements. No

d.c. polarization of the glasses was observed. Fig. 1 shows the relationship between density, d , and annealing time (6–48 h) for $50V_2O_5 \cdot 20SnO \cdot 30TeO_2$ glass; an initial and press-quenched glass density before annealing was 4.012 g cm^{-3} . In Fig. 1, d is shown to increase proportionally with increasing annealing time. Fig. 2 shows the temperature dependence of electrical conductivity, σ , for the glasses of V_2O_5 : SnO: TeO_2 50:20:30, 50:10:40 and 40:10:50 mol % at $T = 200$ –473 K. Changes in the slopes in this relationship are clearly observed at temperatures < 200 K [7]. The data in Fig. 2 was fitted for the relation \ln -

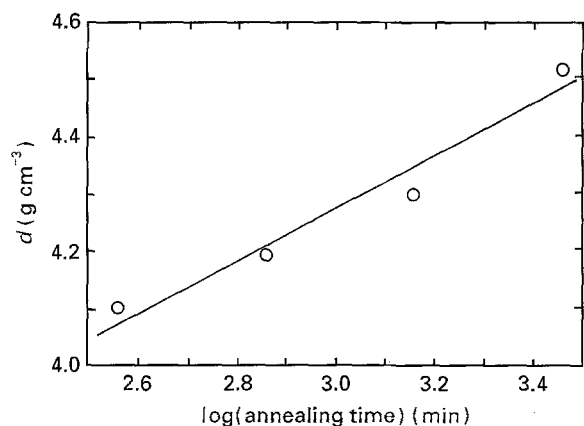


Figure 1 Effect of annealing time on density, d , for $50V_2O_5 \cdot 20SnO \cdot 30TeO_2$ glass. The line is calculated from Equation 8.

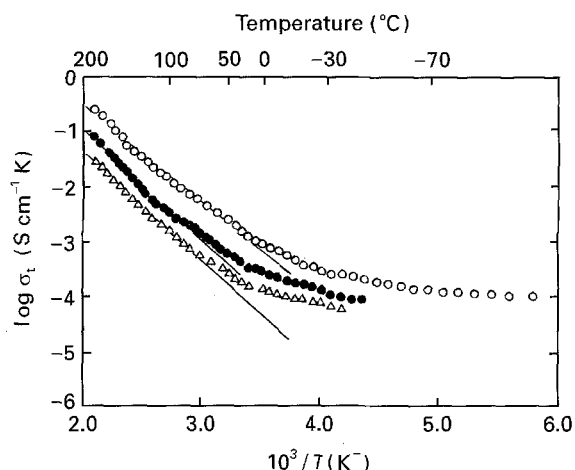


Figure 2 Temperature dependence of d.c. conductivity for annealing the glass system of V_2O_5 -SnO- TeO_2 [7]. Annealing time, 6 h; V_2O_5 : SnO: TeO_2 (mol %), \circ , 50:20:30, \bullet , 50:10:40, \triangle , 40:10:50.

TABLE I Physical parameters of V_2O_5 -SnO- TeO_2 glasses

Compositions (mol %)			Annealing time (h)	C_V	$\nu_0 \exp(-2\alpha R)$ (s^{-1})	$\log \sigma_0$ ($S \text{ cm}^{-1}$)	W_D^a (eV)
V_2O_5	SnO	TeO_2					
50	20	30	48	0.118	2.4×10^{12}	4.0	0.08
50	20	30	24	0.117	2.4×10^{12}	4.0	0.08
50	20	30	12	0.117	2.4×10^{12}	4.0	0.08
50	20	30	6	0.117	2.4×10^{12}	4.0	0.08
50	10	40	6	0.107 ^b	2.6×10^{12}	4.0	0.09
40	10	50	6	0.175 ^b	2.0×10^{11}	2.0	0.09

^a Ref. [7].

^b Ref. [6].

$(\sigma T) \propto T^{-1}$ by the least-square technique between 473 K and RT. For these glasses, the best fit was obtained with $r^2 = 0.9993$ (r is the correlation coefficient) for $R = 2.0 \times 10^{-4} \text{ S cm}^{-1}$ (R is the range) in σ . The relationship between $\log(\sigma T)$ and T^{-1} is linear from RT to 473 K, similar to SPH conduction of the previous glasses [6]. The fraction of the reduced vanadium ion, $C_V = [V^{4+}]/[V^{4+}] + [V^{5+}]$, for $50V_2O_5 \cdot 20SnO \cdot 30TeO_2$ glass was 0.117–0.118 for annealing times from 6 to 48 h, and hardly varied. These C_V values shown in Table I, were the same as those for the non-annealed glass of $50V_2O_5 \cdot 20SnO \cdot 30TeO_2$ ($C_V = 0.117$) [6]. Since the conduction mechanism of these annealed glasses at low temperatures (200 K–RT) has been discussed elsewhere [7], only the conduction at high temperatures (RT–437 K) will be discussed in section 4.1.

4. Discussion

4.1. Electrical conduction for annealed glasses

The electrical conductivity for SPH [12,13] is expressed by:

$$\sigma = \frac{\nu_0 C(1-C)e^2}{kTR} \exp(-2\alpha R) \exp(-W/kT) \quad (1)$$

$$W = W_H + W_D/2, T > \Theta_D/2 \quad (2)$$

$$\sigma_0 = \frac{\nu_0 C(1-C)e^2}{kR} \exp(-2\alpha R) \quad (3)$$

where ν_0 is the optical phonon frequency, R is the average spacing between transition metal ions ($= (1/N)^{1/3}$), N is the transition metal ion density, C is the fraction of reduced transition metal ion ($= C_V$), α is the tunnelling factor, i.e. the rate of the wave function decay, W is the activation energy, W_H is the polaron hopping energy, W_D is the disorder energy, k is the Boltzmann constant, Θ_D is the Debye temperature and σ_0 is the pre-exponential factor.

For the adiabatic region, the tunnelling term, α , in Equation 1 is negligible because the dominant factor contributing to d.c. conductivity was W [3, 6, 14–18]. So, the conductivity is more dependent on concentration of transition metal oxide. Since $\exp(-2\alpha R) \approx 1$,

σ is given by:

$$\sigma_0 = \frac{v_0 C(1-C)e^2}{kR} \exp(-2\alpha R) \exp(-W/kT) \quad (4)$$

In order to confirm $\exp(-2\alpha R) \approx 1$, the transition probability, $v_0 \exp(-2\alpha R)$, in Equation 3 was calculated using experimental values of C_V and R . The result was $v_0 \exp(-2\alpha R) = 1.79 \times 10^{11} - 2.6 \times 10^{12} \text{ s}^{-1}$.

Apart from this, v_0 in $v_0 \exp(-2\alpha R)$ can be calculated using $k\Theta_D = hv_0$ (h is Planck constant) [14–18]. If we assume Θ_D to be several hundred K in the present glasses, considering $\Theta_D = 340\text{--}500 \text{ K}$ for $\text{V}_2\text{O}_5\text{--P}_2\text{O}_5$ [19] and alkaline silicate glasses [20], v_0 is $10^{12}\text{--}10^{13} \text{ s}^{-1}$. These values agree well with the values of $v_0 \exp(-2\alpha R)$ for $\text{V}_2\text{O}_5 \geq 50 \text{ mol } \%$. So, the conduction in this region was attributed to adiabatic SPH because $\exp(-2\alpha R)$ can be regarded as nearly 1, i.e. $\alpha R \approx 0$. When the conduction is due to adiabatic SPH, the term $v_0 C(1-C)e^2/kR$ in Equation 4 is not dependent on V_2O_5 concentration, and hardly varies in different vanadate glasses [3, 6, 14–18]. On the other hand, for $\text{V}_2\text{O}_5 < 50 \text{ mol } \%$, $v_0 \exp(-2\alpha R)$ tended to decrease with decreasing V_2O_5 ; this confirms non-adiabatic SPH conduction.

Further, $\log \sigma_0$ hardly varied for different V_2O_5 concentrations at various annealing times (Table I). However, $\log \sigma_0$ decreased for $\text{V}_2\text{O}_5 < 50 \text{ mol } \%$ and was lower than $\text{V}_2\text{O}_5 \geq 50 \text{ mol } \%$. From this, it is concluded that for $\text{V}_2\text{O}_5 \geq 50 \text{ mol } \%$, hopping conduction is adiabatic, while for $\text{V}_2\text{O}_5 < 50 \text{ mol } \%$, non-adiabatic SPH conduction occurs. In the adiabatic hopping regime, σ should depend only on W [3, 6, 14–18] which results in a linearity between $\log \sigma$ and W from Equation 4, and the slope between $\log \sigma$ and W being equal to $-1/2.303kT$ [3, 6, 14–18].

Fig. 3 shows the relation between $\log \sigma$ and W at 423 K, giving the predicted slope ($-1/2.303kT$) for $\text{V}_2\text{O}_5 \geq 50 \text{ mol } \%$. The slope deviated, however, from $-1/2.303kT$ for $\text{V}_2\text{O}_5 < 50 \text{ mol } \%$. The temperature evaluated from the slope was ca. 423 K, which agreed satisfactorily with the experimental temperature ($T = 423 \text{ K}$). These above discussions, applying the Mott–Austin formula (Equation 1) [12, 13], lead to the conclusion that the conduction of the present glasses was attributable to SPH of electrons.

4.2. Effects of annealing on activation energy

Fig. 4 presents the relationship between W and annealing time. W decreased with an increase in annealing time. The relationship between σ and annealing time (0–48 h) for $50\text{V}_2\text{O}_5\cdot 20\text{SnO}\cdot 30\text{TeO}_2$ glass is shown in Fig. 5. From Fig. 5, σ , at 473 and 463 K was 3.98×10^{-4} and $3.16 \times 10^{-4} \text{ S cm}^{-1}$, respectively, i.e. little variation with temperature. However, at 423 K ranged from 1.12×10^{-4} to $1.58 \times 10^{-4} \text{ S cm}^{-1}$ for annealing from 6 to 48 h, i.e. increased with annealing time; this was attributable to a decrease in

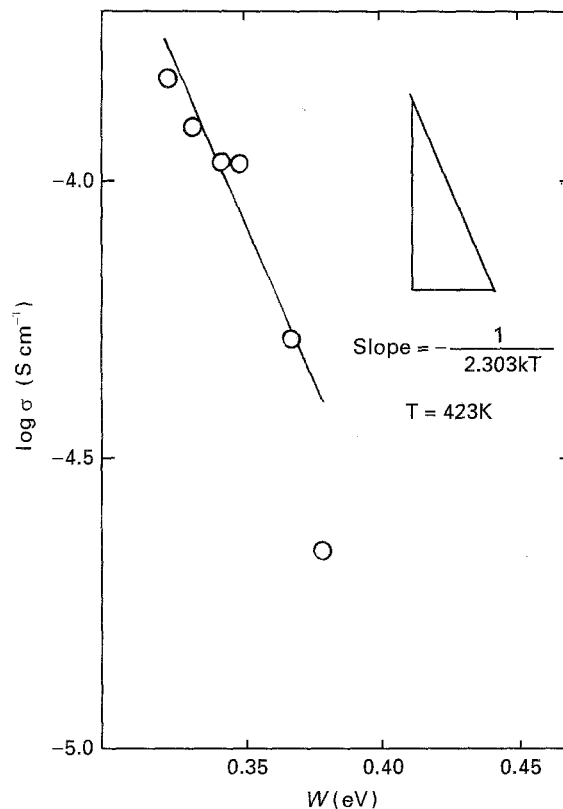


Figure 3 Relationship between $\log \sigma$ at 423 K and W for annealed glasses of the $\text{V}_2\text{O}_5\text{--SnO--TeO}_2$ system.

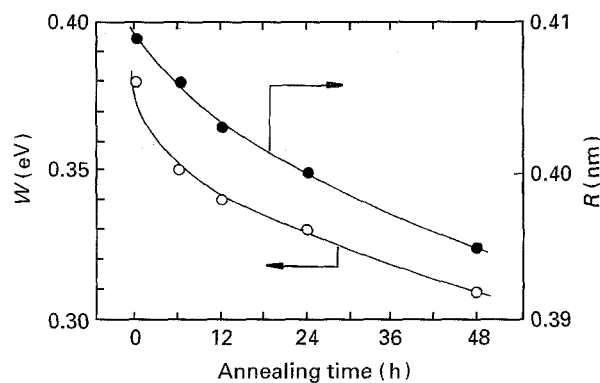


Figure 4 Effect of annealing time on W and R for $50\text{V}_2\text{O}_5\cdot 20\text{SnO}\cdot 30\text{TeO}_2$ glass. The lines are drawn as a guide for the eyes.

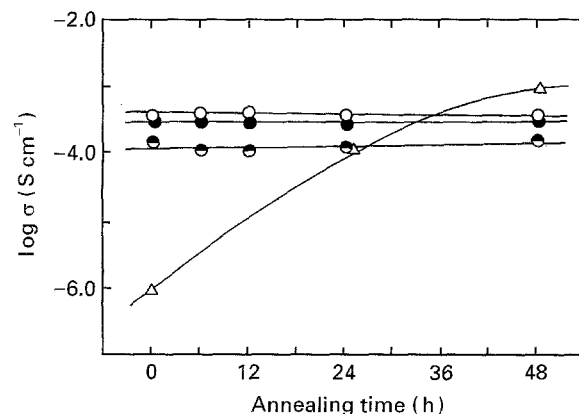


Figure 5 Effect of $\log \sigma$ on annealing time. Temperature (K): \circ , 473; \bullet , 463; \ominus , 423. \triangle , $50\text{Nb}_2\text{O}_5\cdot 20\text{V}_2\text{O}_5\cdot 30\text{TeO}_2$ glass [8]. The lines are drawn as a guide for the eyes.

W ($= 0.35-0.31$ eV) which decreased with increasing annealing time (Fig. 4). σ of the crystallized glass from $50\text{Nb}_2\text{O}_5 \cdot 20\text{V}_2\text{O}_5 \cdot 30\text{P}_2\text{O}_5$ (mol %) [9] gave $\sigma 10^{-6}-10^{-3} \text{ S cm}^{-1}$ for annealing from 0 to 48 h. This remarkable increase in σ was considered to be due to crystallization of the glass with increasing annealing time at 973 K. In comparison to the present glass ($50\text{V}_2\text{O}_5 \cdot 20\text{SnO} \cdot 30\text{TeO}_2$ glass) with the crystallized glass of $50\text{Nb}_2\text{O}_5 \cdot 20\text{V}_2\text{O}_5 \cdot 30\text{P}_2\text{O}_5$ [9], the changes in σ for the present glass were less than that of $50\text{Nb}_2\text{O}_5 \cdot 20\text{V}_2\text{O}_5 \cdot 30\text{P}_2\text{O}_5$ glass, indicating that the effect of the annealing period on σ is rather small for non-crystallized glasses.

The effect of the heat treatments on W will now be discussed. The glass density, d , increased with an increase in annealing time (Fig. 1), i.e. the glass structure became more closely packed. So, as a measure of the glass structure, the oxygen ion molar volume of the glass (V_0^*) [6, 16–18, 21–23] is evaluated as:

$$V_0^* = \frac{(M_{\text{V}_2\text{O}_5} - 16C_V)X + M_{\text{TeO}_2}Y + M_{\text{SnO}}Z}{d[(5 - C_V)X + 2Y + Z]} \quad (5)$$

where M is molecular weight; X , Y and Z are mole fractions of V_2O_5 , TeO_2 and SnO , respectively; d is density of the glass; C_V is the fraction of reduced transition metal ion; $C_V = [\text{V}^{4+}]/[\text{V}^{4+}] + [\text{V}^{5+}]$.

Fig. 6 shows the relationship V_0^* versus annealing time for $50\text{V}_2\text{O}_5 \cdot 20\text{SnO} \cdot 30\text{TeO}_2$ glass. In this figure, V_0^* decreased with an increase in annealing period, signifying that the glass structure became more closely packed with longer annealing times. This result suggests a decrease in the mean distance between V ions, R , with annealing. The relationship between R , calculated from the glass density, and annealing time is shown in Fig. 4. In fact, R became smaller with increase in annealing times.

It is known that R generally affects the polaron band width, J [6, 15, 16], in SPH. For adiabatic SPH, W using J [24–26], is given by:

$$W - 1/2W_D \simeq W_H = 1/2W_P = 1/2(W_{P'} - 2J) \quad (6)$$

where $W_{P'}$ is the maximum polaron energy ($1/2W_{P'} = 0.44$ eV [6]), W_P is the polaron binding

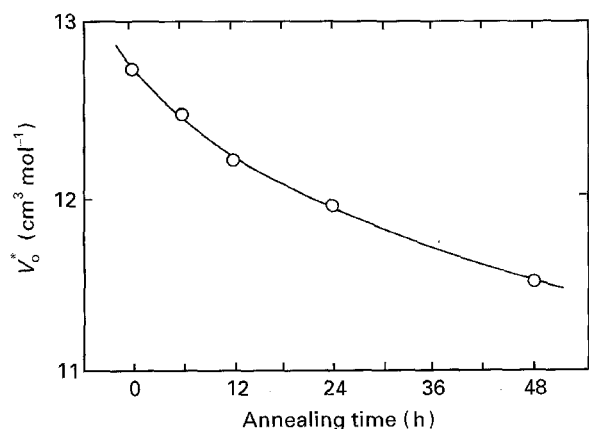


Figure 6 Effect of annealing time on oxygen molar volume, V_0^* for $50\text{V}_2\text{O}_5 \cdot 20\text{SnO} \cdot 30\text{TeO}_2$ glass. The line is drawn as a guide for the eyes.

energy. In contrast, for non-adiabatic SPH, W is described [24–26] as:

$$W - 1/2W_D \simeq W_H = 1/2W_{P'} \quad (7)$$

W_D was estimated to be 0.08–0.09 eV using the experimental data in Table I obtained from the conductivity measurements at low temperatures [7]. We also calculated W_H with W_D and estimated J using Equation 5. Fig. 7 shows the relationship between J and annealing time, presenting an increase in J with an increase in annealing time. This increase in J means an easy hopping [6, 16, 17]. Besides, the W_H –annealing time relation described in Fig. 7 denotes that W_H lowered with an increase in J and in the annealing period. From the above discussion, it is inferred that an increase in annealing time causes a change in glass structure, from a loosely packed to a closely packed one, resulting in a decrease in R . As a result, W lowered because the increase in J led to a decrease in W_H .

4.3. Effects of annealing on density

Next we discuss the effect of annealing on glass density. Mine [27] studied annealing effects on the density of soda–lime–silica glasses and gave the experimental relationship for density change with annealing time as follows:

$$d(t) = d_0 + \text{const} \times \log t \quad (8)$$

where d_0 is initial density of glass at $t = 0$ min, and t is the annealing time (min). Providing that Equation 8 is applicable to the present glasses, the relationship between d and $\log t$ should be proportional. After the best fit of the data (from Fig. 1 for $50\text{V}_2\text{O}_5 \cdot 20\text{SnO} \cdot 30\text{TeO}_2$ glass) for Equation 8, we obtained $r^2 \simeq 0.9540$ (r is the correlation coefficient), a slope (const in Equation 8) of $0.454 (\text{g cm}^{-3} \text{ min}^{-1})$ and $d_0 = 2.9149 \text{ cm}^{-3}$. This d_0 value was, however, different from the experimental d_0 ($d_0 = 4.0149 \text{ cm}^{-3}$, see Section 3). Accordingly, we conclude that the Mine's formula is not applicable to the present glass.

Effects of annealing time on refractive index of glasses have been extensively studied [28–30]. According to Winter [28], the variations in the refractive

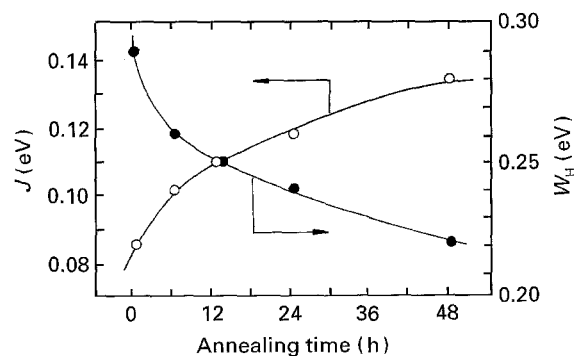


Figure 7 Effect of annealing time on the electronic overlap integral and hopping energy, W_H , for $50\text{V}_2\text{O}_5 \cdot 20\text{SnO} \cdot 30\text{TeO}_2$ glass. \circ , The electronic overlap integral, J ; \bullet , hopping energy, W_H . The lines are drawn as a guide for the eyes.

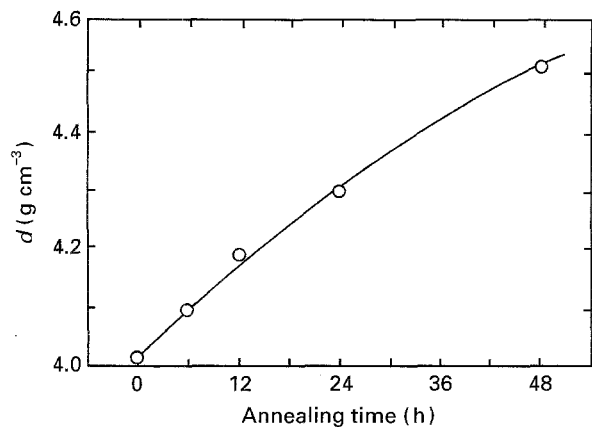


Figure 8 The relationship between density and annealing time for $50\text{V}_2\text{O}_5\cdot 20\text{SnO}\cdot 30\text{TeO}_2$ glass. The line is calculated from Equation 12.

index of optical glasses with annealing time (h) in the α -state, i.e. the state named at $T \leq T_g$, and the β -state, i.e. that at $T > T_g$, were expressed by the following formulae:

$$n = n_T + (n_\alpha - n_T)e^{-Dt} \quad (9)$$

$$n = n_T - (n_\beta - n_T)e^{-Bt} \quad (10)$$

where n_T is the maximum refractive index, n_α and n_β are the initial refractive indexes, for α - and β -states, respectively, and, D and B are constants. Winter's empirical formulae can be transformed to a density-annealing time relationship using Gladston and Dale's formula [31] between n and d described as:

$$r = \frac{n - 1}{d} \quad (11)$$

where r is a constant and not influenced by annealing time.

Since the present glass was under the α -state, we have, combining Equation 9 with $n = rd - 1$ from Equation 11:

$$d = d_T + (d_\alpha - d_T)e^{-Dt} \quad (12)$$

where d_T is the maximum density and d_α the initial density. The relationship between d and t is shown in Fig. 8. In Fig. 8, d_T and D were determined using experimental $d_\alpha = 4.014 \text{ g cm}^{-3}$ so as to obtain the best fit of the experimental data of the density in Fig. 1 for Equation 12, which resulted in a maximum r^2 value of 0.9978. Finally, we obtained $d_T = 5.062 \text{ g cm}^{-3}$ and $D = 0.014 \text{ h}^{-1}$. Good agreements were found in Fig. 8 between the experimental density data (open circles in Fig. 8) and the theoretical curve (solid line) (Equation 12) of the best fit. Accordingly, it is concluded that the effects of annealing time on the density of the present $50\text{V}_2\text{O}_5\cdot 20\text{SnO}\cdot 30\text{TeO}_2$ glass was adequately explained by Winter's formula.

5. Conclusion

Effects of annealing on d.c. conductivity of $\text{V}_2\text{O}_5\text{-SnO-TeO}_2$ glasses prepared by press-quenching were investigated. Density of $50\text{V}_2\text{O}_5\cdot 20\text{SnO}\cdot 30\text{TeO}_2$ glass increased with increasing annealing

time. The conduction for these glasses at 473 K-RT suggested that they are n-type semiconductors, attributed to adiabatic SPH for $\text{V}_2\text{O}_5 \geq 50 \text{ mol } \%$, and to non-adiabatic SPH for $\text{V}_2\text{O}_5 < 40 \text{ mol } \%$. The mechanism of the SPH conduction was not affected by post-annealing. Besides, the conductivity was virtually unchanged by annealing. However, variations in oxygen ion molar volume of the glasses, V_0^* , with annealing time inferred a change in glass structure, i.e. loosely packed to a closely packed structure. As a result, irrespective of no appreciable changes in σ , the values of R , J and W_H varied with annealing. Behaviour of the changes in the density of the glass during annealing was adequately explained by Winter's formula.

References

1. K. SHIMAKAWA, *Phil. Mag.* **60** (1989) 377.
2. H. HIRASHIMA, *Seramikkusu-Ronbun-Shi* **97** (1989) 400.
3. H. MORI, T. KITAMI and H. SAKATA, *J. Non-Cryst. Solids* **168** (1994) 157.
4. L. MURAWSKI, C. H. CHUNG and J. D. MACKENZIE, *ibid.* **32** (1979) 91.
5. N. LEBRUN, M. LÉVY and J. L. SOUQUET, *Solid State Ionics* **40/41** (1990) 718.
6. H. MORI, J. IGARASHI and H. SAKATA, Unpublished work.
7. H. MORI, K. GOTOH and H. SAKATA, *J. Non-Cryst. Solids* **183** (1995) 122.
8. N. F. MOTT, *Phil. Mag.* **19** (1969) 835.
9. T. YOSHIDA, Y. MATSUNO and T. KASHINO, *Nippon Kagakukai Shi* **10** (1981) 1589.
10. H. SAKATA, M. AMANO, T. ISHIGURO and T. HIRAYAMA, *J. Ceram. Soc. Jpn* **100** (1992) 1398.
11. M. AMANO, H. SAKATA, K. TANAKA and T. HIRAYAMA, *ibid.* **102** (1994) 424.
12. N. F. MOTT, *Adv. Phys.* **16** (1967) 49.
13. I. G. AUSTIN and N. F. MOTT, *ibid.* (1969) 41.
14. H. HIRASHIMA, M. MITSUHASHI and T. YOSHIDA, *Yogo-Kyokai-Shi* **90** (1982) 411.
15. H. HIRASHIMA and T. KAWAGUCHI, *Seramikkusu-Ronbun-Shi* **97** (1989) 1144.
16. H. MORI, T. KITAMI and H. SAKATA, *J. Ceram. Soc. Jpn* **101** (1993) 343.
17. H. MORI, J. IGARASHI and H. SAKATA, *ibid.* **101** (1993) 1351.
18. H. HIRASHIMA, H. KUROKAWA, K. MIZOBUCHI and T. YOSHIDA, *Glastech. Ber.* **61** (1988) 151.
19. M. B. FIELD, *J. Appl. Phys.* **40** (1969) 2628.
20. H. NASU, K. HIRAO and N. SOGA, *J. Am. Ceram. Soc.* **64** (1981) C-63.
21. H. HIRASHIMA and H. TANAKA, *Seramikkusu-Ronbun-Shi* **97** (1990) 1150.
22. T. NAITOH, T. NAMEKAWA, A. KATOH and K. MAEDA, *J. Ceram. Soc. Jpn* **100** (1992) 685.
23. C. F. DRAKE, J. A. STEPHAN and B. YATES, *J. Non-Cryst. Solids* **28** (1978) 61.
24. T. HOLSTEIN, *Ann. Phys. (NY)* **8** (1959) 325.
25. L. FRIEDMAN and T. HOLSTEIN, *ibid.* **21** (1963) 494.
26. M. SAYER and A. MANSINGH, *J. Non-Cryst. Solids* **58** (1983) 91.
27. M. MINE, *Yogyo-Kyokai-Shi* **63** (1955) 692.
28. A. WINTER, *J. Am. Ceram. Soc.* **26** (1943) 193.
29. A. Q. TOOL and E. E. HILL, *J. Soc. Glass Tech., Trans* **9** (1925) 185.
30. H. A. McMASTER, *J. Am. Ceram. Soc.* **28** (1945) 1.
31. I. H. GLADSTONE and T. P. DALE, *Phil. Trans.* (1863) 337.

Received 16 June 1994
and accepted 5 April 1995